

**SCHOOL OF MATERIALS AND MINERAL RESOURCES ENGINEERING
UNIVERSITI SAINS MALAYSIA**

**INVESTIGATION OF ENCAPSULANT DISCOLORATION MECHANISM IN
UV/BLEU LIGHT-EMITTING DIODE WITH COPPER HYBRID PARTICLES
FILLER USING TAGUCHI METHOD**

By

CHRISTINA CHIN KAI QI

Supervisor: Dr. Sivakumar A/L Ramakrishnan

Co-Supervisor: Assoc. Prof. Ir. Dr. Pung Swee Yong

Dissertation submitted in partial fulfillment
of the requirements for the degree of Bachelor of Engineering with Honours
(Materials Engineering)

UNIVERSITI SAINS MALAYSIA

19 AUGUST 2022

DECLARATION

I hereby declare that I have conducted, completed the research work and written the dissertation entitled “**Investigation Of Encapsulant Discoloration Mechanism in Uv/Blue Light-Emitting Diode With Copper Hybrid Particles Filler Using Taguchi Method**”. I also declare that it has not been previously submitted for the award for any degree or diploma or other similar title of this for any other examining body or University.

Name of Student : Christina Chin Kai Qi

Signature:

Date : 19 August 2022

Witnessed by

Supervisor : Dr. Sivakumar A/L Ramakrishnan

Signature:

Date : 19 August 2022

Co-Supervisor : Assoc. Prof. Ir. Dr. Pung Swee Yong

Signature:

Date : 19 August 2022

ACKNOWLEDGEMENTS

First and foremost, I would like to express my appreciation to my supervisor, Dr. Sivakumar A/L Ramakrishnan for his invaluable advice and support to me in this project. His understanding and passion towards the world of mathematics has enlighten me throughout this project. I truly thankful that he guided and encouraged me along the journey of completing this thesis work. Besides, this thesis would noy have been possible without my co-supervisor, Assoc. Prof. Ir. Dr. Pung Swee Yong. He has been a good counsel which enables me to develop an understanding on the experimental and thesis work. His intuition and perception always inspired me to lead the project come to fruition. I would also like to thank Prof. Ir. Dr. Mariatti binti Jaafar Mustapha for generously providing grant (grant number: 308 AIBAHAN 415403) to make this project more successful.

At the same time, I would like to express the deepest gratitude to School of Materials and Mineral Resources Engineering, School of Chemical Sciences, Centre for Global Archaeological Research, Universiti Sains Malaysia (USM), Puan Haslina binti Zulkifli, Encik Mohammad Azrul bin Zainol Abidin and Encik Mohamad Syafiq bin Mustapha Sukri for providing required apparatus, equipment and laboratory to me in conducting and completing my project. Without the assistance from the technical staffs, this project would not be carried out smoothly. Their technical knowledge and experience greatly aid me to accomplish the project within a short period of time.

Furthermore, I would like to acknowledge my family and friends for helping me throughout this project. The unconditional love and moral support of theirs have been giving me patience and determination to complete this project within the time frame.

TABLE OF CONTENTS

DECLARATION	ii
ACKNOWLEDGEMENTS	iii
LIST OF TABLES	vi
LIST OF FIGURES	vii
LIST OF ABBREVIATIONS	ix
LIST OF SYMBOLS	xi
ABSTRAK.....	xii
ABSTRACT.....	xiii
CHAPTER 1	1
1.1 Background.....	1
1.2 Problem Statement.....	3
1.3 Research Objectives.....	4
1.4 Scopes of Research	4
1.5 Dissertation Outline	5
CHAPTER 2	6
2.1 LED.....	6
2.1.1 Working Principle of LED.....	9
2.1.2 Encapsulant embedded in LED.....	10
2.1.3 Yellowing/Browning (Discoloration) of LED Encapsulant	14
2.2 Basics of TiO ₂	15
2.3 Performance of TiO ₂ Particles as Filler in the LED Encapsulant.....	19
2.3.1 Photocatalytic Activity of TiO ₂	21
2.4 Surface Modification of TiO ₂	25
2.4.1 Formation of Cu/TiO ₂ Particles via Doping	30
2.5 Taguchi Method	33
CHAPTER 3	34
3.1 Introduction.....	34
3.2 Raw Materials	37
3.3 Experimental Procedure.....	37
3.4 Characterization Techniques.....	39

3.4.1	FESEM.....	40
3.4.2	EDX	40
3.4.3	XRD	41
3.4.4	Zeta Potential Measurement	42
3.5	Optical Energy Band Gap and Photocatalytic Performance	43
3.6	DOE via Taguchi Method.....	44
CHAPTER 4		46
4.1	Synthesis and Characterization of Cu/TiO ₂ Particles	46
4.1.1	FESEM with EDX Analysis	46
4.1.2	XRD Results	54
4.1.3	Zeta Potential Measurement	56
4.1.4	Optical Energy Band Gap	57
4.1.5	Photocatalytic Properties	59
4.2	Local Optimization of Photocatalytic Performance of Cu/TiO ₂ Particles	64
4.3	Characterization of Silicone Thin Films	70
CHAPTER 5		72
5.1	Conclusion	72
5.2	Recommendations for Future Work.....	73
REFERENCES		74
APPENDIX A.....		84
APPENDIX B		85
APPENDIX C		86
APPENDIX D.....		89

LIST OF TABLES

	Page
Table 2.1: Failure modes of LEDs.....	8
Table 2.2: Comparison of the properties of silicone resin and epoxy resin.....	13
Table 2.3: Properties of the TiO ₂ polymorphs.....	18
Table 2.4: Factors influencing the photocatalytic efficiency.....	24
Table 2.5: Methods of modification to improve the photocatalytic performance and their respective improvements and drawbacks.....	28
Table 3.1: List of raw materials used for this project.....	36
Table 3.2: Amount of raw materials used to prepare metal solution.....	37
Table 3.3: 3 factors and 3 levels in L9 array Taguchi design.....	43
Table 3.4: List of L9 array conditions of Cu/TiO ₂ particles.....	44
Table 4.1: Surface morphology of L9 array conditions of Cu/TiO ₂ particles at 30 kX magnification.....	47
Table 4.2: Average particle size of the TiO ₂ _WA, TiO ₂ _A and L9 array conditions of Cu/TiO ₂ particles.....	50
Table 4.3: List of experimental data of Cu/TiO ₂ particles collected via Taguchi method.....	64
Table 4.4: Response table of k for S/N ratio.....	65
Table 4.5: Response table of PE for S/N ratio.....	65
Table 4.6: L9 orthogonal array with calculation for k.....	68
Table 4.7: Mean k of factors and level combination.....	68
Table 4.8: L9 orthogonal array with calculation for PE.....	69
Table 4.9: Mean PE of factors and level combination.....	69

LIST OF FIGURES

	Page
Figure 2.1: Working principle of LED.....	10
Figure 2.2: Cross-sectional view of high-power white LED.....	11
Figure 2.3: Different crystal structure of TiO ₂ polymorphs: (a) anatase, (b) rutile, and (c) brookite.....	17
Figure 2.4: LED encapsulant: (a) silicone and (b) TiO ₂ doped silicone.....	21
Figure 2.5: Durability test for the LED module with different packages under 85 °C/85 % RH condition.....	21
Figure 2.6: Schematic diagram of photocatalysis.....	23
Figure 2.7: Various reactions involved in TiO ₂ photocatalysis.....	23
Figure 2.8: Trade-off between co-catalyst loading (dopant concentration) and reaction rate (photocatalytic activity).....	32
Figure 3.1: Overall flowchart of this project.....	35
Figure 3.2: Temperature profile of annealing process.....	37
Figure 4.1: FESEM image of (a) TiO ₂ _WA and (b) TiO ₂ _A particles at 30 kX magnification.....	46
Figure 4.2: Comparison of particle size with TiO ₂ _WA, TiO ₂ _A and L9 array conditions of Cu/TiO ₂ particles.....	51
Figure 4.3: At % of Ti and O present in TiO ₂ particles.....	52
Figure 4.4: At % of Cu present in L9 array conditions of Cu/TiO ₂ particles.....	53
Figure 4.5: XRD pattern of TiO ₂ _WA and TiO ₂ _A particles.....	54
Figure 4.6: XRD patterns of the L9 array conditions of Cu/TiO ₂ particles.....	55
Figure 4.7: Zeta potential of the L9 array conditions of TiO ₂ and Cu/TiO ₂ particles.....	56

Figure 4.8: Absorption spectra of (A) TiO ₂ _WA and TiO ₂ _A particles and (b) L9 array conditions of Cu/TiO ₂ particles. (C) Onset absorption peak of the TiO ₂ _WA, TiO ₂ _A and L9 array conditions of Cu/TiO ₂ particles.....	57
Figure 4.9: Tauc plot for the TiO ₂ _WA, TiO ₂ _A and L9 array conditions of Cu/TiO ₂ particles....	58
Figure 4.10: Absorption spectra of 5 ppm RhB solution before UV irradiation.....	59
Figure 4.11: Graph of (a) absorbance versus UV irradiation time and (b) wavelength versus UV irradiation time of TiO ₂ _WA and TiO ₂ _A particles.....	60
Figure 4.12: Graph of (a) absorbance versus UV irradiation time and (b) wavelength versus UV irradiation time of the L9 array conditions of Cu/TiO ₂ particles.....	61
Figure 4.13: Graph of (a) PE of RhB solution with the presence of the L9 array conditions of Cu/TiO ₂ particles and (b) PE of the L9 array conditions of Cu/TiO ₂ particles after 120 minutes of UV irradiation.....	62
Figure 4.14: (a) 1st kinetic order plot and (b) k of the L9 array conditions of Cu/TiO ₂ particles under UV irradiation.....	62
Figure 4.15: Probability plot of k and PE.....	64
Figure 4.16: Main effect plots of S/N ratio for (a) k and (b) PE.....	66
Figure 4.17: Normal probability plots of S/N ratio for (a) k and (b) PE.....	67

LIST OF ABBREVIATIONS

ANOVA	Analysis of Variance
CB	Conduction Band
Cu	Copper
CuO	Copper Oxide
Cu/TiO ₂	Copper Hybrid Particles
DOE	Design of Experiment
e ⁻	Negatively Charged Electron
et. al.	et alia
E _{cb}	Conduction Band Edge
E _{vb}	Valence Band Edge
EDX	Energy Disperse X-ray spectroscopy
FESEM	Field-Emission Scanning Electron Microscope
h ⁺	Positively Charged Hole
H ₂	Hydrogen
HRTEM	High-Resolution Transmission Electron Microscopy
hν	Photon Energy
ICSD	Inorganic Crystal Structure Database
i.e.	id est
k	Rate Constant
N ₂	Nitrogen
LED	Light Emitting Diode
LEE	Light Extraction Efficiency

O	Oxygen
PE	Photodegradation Efficiency
RhB	Rhodamine B
SCFH	Standard Cubic Feet per Hour
Ti	Titanium
TiO ₂	Titanium Dioxide
USD	United States Dollar
UV	Ultra-violet
VB	Valence Band
XRD	X-Ray Diffraction

LIST OF SYMBOLS

a.u.	Arbitrary Unit
At %	Atomic Percent
°	Degree
°C	Degree Celsius
eV	Electronvolt
nm	Nanometer
rpm	Rotation per Minute
%	Percent

**PENYIASATAN MEKANISME PERUBAHAN WARNA ENKAPSULAN DALAM DIOD
PEMANCAR CAHAYA UV/BIRU DENGAN PENGISI ZARAH HIBRID KUPRUM
MENGUNAKAN KAEDAH TAGUCHI**

ABSTRAK

Zarah titanium dioksida (TiO_2) dikenali sebagai semikonduktor yang menjanjikan kerana prestasinya yang tinggi dalam aplikasi fotokatalitik. Walau bagaimanapun, ia tidak mempunyai kestabilan apabila terdedah kepada cahaya ultra ungu (UV) secara lama-lama. Projek ini memberi tumpuan kepada prestasi fotomangkkin zarah hibrid kuprum (Cu/TiO_2) di mana mekanisme perubahan warna enkapsulan dalam UV/Blue Light-Emitting Diod (LED) boleh dipertingkatkan dengan memasukkan zarah Cu/TiO_2 dalam LED sebagai pengisi. Kuprum (Cu) dimendapkan pada permukaan zarah TiO_2 melalui kaedah impregnasi dengan sinaran UV dan kesan tiga parameter sintesis, iaitu kepekatan ion Cu^{2+} , masa penyinaran UV dan suhu penyepuhlindungan telah dikaji. Analisis struktur dan morfologi menunjukkan bahawa pemendapan Cu pada permukaan zarah TiO_2 . Analisis metunjukkan bahawa zarah Cu/TiO_2 _1 (disintesis dengan 300 ppm ion Cu^{2+} , 120 minit penyinaran UV dan suhu penyepuhlindungan 550 °C) mempunyai pemalar kadar terendah (k) 0.000278 min^{-1} dan kecekapan fotodegradasi (PE) sebanyak 3.44098 % pada 120 minit. Pengoptimuman parameter sintesis telah dijalankan melalui kaedah Taguchi untuk mencapai degradasi fotokatalitik zarah Cu/TiO_2 yang paling lemah. Parameter sintesis optimum yang diperolehi ialah 300 ppm ion Cu^{2+} , 0 minit penyinaran UV dan suhu penyepuhlindungan 400 °C. Tambahan pula, kesan kekuningan selepas pendedahan di bawah penyinaran UV telah diperhatikan dan didapati bahawa kesan kekuningan pada filem silikon nipis yang digabungkan dengan zarah Cu/TiO_2 adalah lebih rendah berbanding dengan yang digabungkan dengan zarah TiO_2 . Akibatnya, zarah Cu/TiO_2 boleh mengurangkan aktiviti fotolitik yang mengakibatkan pemotongan rantai dan terurai dengan kekuningan. Oleh itu, zarah Cu/TiO_2 boleh dibenamkan dalam enkapsulan LED sebagai pengisi untuk mengurangkan kemerosotan fotokatalitik degradasi serta mencapai kecekapan pengekstrakan cahaya (LEE) yang lebih besar.

INVESTIGATION OF ENCAPSULANT DISCOLORATION MECHANISM IN UV/BLUE LIGHT-EMITTING DIODE WITH COPPER HYBRID PARTICLES FILLER USING TAGUCHI METHOD

ABSTRACT

Titanium dioxide (TiO₂) particles is known to be a promising semiconductor due to its high performance in photocatalytic applications. However, with prolonged exposure to ultraviolet (UV) light, it loses its stability. This project focus on the photocatalytic performance of copper hybrid (Cu/TiO₂) particles where the encapsulant discoloration mechanism in UV/Blue Light-Emitting Diode (LED) can be improved by incorporating Cu/TiO₂ particles in the LED as the filler. Copper (Cu) was deposited on the surface of TiO₂ particles through impregnation method assisted by UV radiation and the effect of three synthesis parameters i.e. concentration of Cu²⁺ ions, irradiation time and annealing temperature were studied. The structural and morphological analysis indicated that the deposition of Cu on the surface of TiO₂ particles. It was shown that the Cu/TiO₂_1 particles (synthesized with 300 ppm of Cu²⁺ ions, 120 minutes of UV irradiation and annealing temperature of 550 °C) has the lowest rate constant (k) of 0.000278 min⁻¹ and photodegradation efficiency (PE) of 3.44098 % at 120 minutes. The optimization of synthesis parameters was employed via Taguchi method to achieve poorest photocatalytic degradation of Cu/TiO₂ particles. The finding shows that the optimal synthesis parameters obtained were 300 ppm of Cu²⁺ ions, 0 minute of UV irradiation and annealing temperature of 400 °C. Furthermore, the yellowing effect after exposure under UV irradiation was observed and it is found that the yellowing effect on the thin silicone film incorporated with Cu/TiO₂ particles were lesser as compared to the thin silicone film incorporated with TiO₂ particles. As a result, Cu/TiO₂ particles can reduce the photodegradation activity that may cause the polymeric material in the LED encapsulant being degraded through chain scission and turned yellowish. Therefore, it is said that Cu/TiO₂ particles can be embedded in the LED encapsulant as filler to reduce the photocatalytic degradation as well as achieve greater light extraction efficiency (LEE).

CHAPTER 1

INTRODUCTION

In this project, Cu/TiO₂ particles were synthesised using impregnation method assisted by UV light. Taguchi analysis were implemented to optimise the photocatalytic properties of Cu/TiO₂ particles through modifying the synthesis parameters including the concentration of Cu²⁺ ions solution, UV irradiation time and annealing temperature to get the poorest photocatalytic degradation. This chapter explains the research background, problem statement, research objectives, scope of research and dissertation outline.

1.1 Background

Among various challenges for LEDs, LEE and light output degradation are the main issues when it comes to the lifetime and reliability (Yazdan et al., 2018). The majority of LED failures are related to LED packaging, which ultimately results in colour shift, optical degradation and discolouration of encapsulant materials, carbonisation of silicone encapsulant and thermal quenching of phosphor happened (Yazdan et al., 2018; Yazdan et al., 2020). These failures are commonly due to the ageing of polymeric materials, which is a result of poor heat dissipation performance due to high working temperature (Zhao et al., 2022; Lin et al., 2020; Zhou et al., 2022). Besides high working temperature, constant and long exposure to UV radiation is also the key factors of photodegradation that leads to discolouration and yellowing. Therefore, important technical issues such as increasing LEE, minimizing heat generation, enhance heat dissipation performance and making the LED packaging more heat and UV resistance are required to be considered for future developments (Yazdan et al., 2018). A promising LED packaging should be having a high refractive index, strong mechanical strength, strong adhesion and bond strength, stable microstructure and high resistance against chemical attack and UV radiation (Yazdan et al., 2020).

Polymeric materials were thought to be a potential material to be integrated into LED packaging because they offer substantial cost reduction, room temperature processing, and good flexibility (Baillot et al., 2015). The LED encapsulant is typically made of silicone, that serves as an optical medium surrounding the LED die to isolate against structural, mechanical and chemical stresses from the outside environment and also contributes to extraction of generated photons (Appaiah et al., 2015). The silicone encapsulant possess good UV resistance but they have limited RI (about 1.4 to 1.5), the large RI difference between silicone encapsulation and LED chips eventually leads to light scattering and thus low LEE of LEDs is observed (Wang et al., 2014; Li et al., 2008). Modifications on encapsulant material is then studied accordingly with the incorporation of dopants into silicone resins (Huang *et al.*, 2015).

According to several studies, researchers have incorporated TiO₂ particles as the filler in the silicone resins due to its high refractive index which tend to increase the refractive index of polymer matrix (Li et al., 2008). Most of the polymeric resins have an adjustable range of refractive index, for instance, approximately 1.3 to 1.7, while the TiO₂ particles have a high refractive index of 2.45 to 2.7. With the incorporation of TiO₂ particles into the polymeric resins for about 60 wt %, an increment in the refractive index was observed from 1.5 up to 1.8 (Tao et al., 2011). TiO₂ is known to be a promising semiconductor due to its high performance in photocatalytic applications. It is a stable, efficient and green photocatalytic material which portrays chemical inertness, corrosion resistance, high reactivity and excellent charge transport ability (Janczarek & Kowalska, 2017; Perarasan et al., 2021). However, pristine TiO₂ has a wide band gap, with a range of 3.0 eV – 3.2 eV, causing it to portray high band gap energy, high recombination charge rate and low quantum yield, which leads to limited practical application (Qaderi et al., 2021). Although TiO₂ has great photocatalytic properties, it lacks stability upon exposure to UV light for long hours. It is believed that introduction of doping elements to TiO₂ is beneficial for increment of stability. Several improvements such as doping, surface modification, semiconductor coupling and dye sensitization

have been proposed in order to select the optimum approach for greater photogeneration efficiency (Janczarek & Kowalska, 2017).

In this research, Cu was deposited on TiO₂ particles through impregnation method assisted by UV radiation, using various concentration of Cu²⁺ ions (100, 200 and 300 ppm), irradiation time (0, 15 and 120 minutes) and annealing temperature (400, 550 and 700 °C). The main aim of this research is reviewing the effect of synthesis parameters on the photodegradation efficiency of silicone encapsulant. Several characterizations were done to study the photocatalytic properties, following with application of DOE via Taguchi method to optimize (poorest photocatalytic efficiency) the photocatalytic degradation of Cu/TiO₂ particles by varying the synthesis parameters.

1.2 Problem Statement

This work is addressed to following problems:

1. Photocatalytic degradation of LED encapsulant caused the yellow/browning (discoloration) of LED encapsulant.

Under common operating conditions, LEDs optical performance can be limited by optical and thermal failure mechanisms due to the aging of the optical materials which influenced the polymer molecular structure (Baillot et al., 2015; Fan et al., 2021). Thermal oxidation is the crucial mechanism which leads to the polymer encapsulant materials to degrade via chemical degradation upon exposure of elevated temperatures (Yazdan et al., 2020; Singh & Tan, 2018; Appaiah et al., 2015). This phenomenon will cause encapsulant materials to turn discoloured, which will eventually result in an enhanced absorption of blue light (Yazdan et al., 2020). At the same time, photodegradation that caused discolouration of encapsulant depends on the exposure duration and intensity of radiation (Yazdan et al., 2020). The inconsistent degradation of wavelength-dependent transmittance caused the nature of

oxidation process have a drop of the blue/yellow light intensity ratio, where the colour shift occurs toward yellow field (Lu et al., 2015).

1.3 Research Objectives

The objectives of this research project are:

1. To synthesize and characterize Cu/TiO₂ particles by impregnation method assisted by UV light.
2. To optimize (poorest photocatalytic efficiency) the photocatalytic degradation of Cu/TiO₂ particles by varying synthesis parameters such as concentration of Cu²⁺ ions solution, UV irradiation time and annealing temperature.

1.4 Scopes of Research

This work includes two phases. In first phase, Cu/TiO₂ particles was synthesised by depositing Cu on TiO₂ particles with impregnation method assisted by UV irradiation. The synthesis parameters such as concentration of Cu²⁺ ions solution, UV irradiation time and annealing temperature were varied to investigate the effect of these parameters on the photocatalytic properties of Cu/TiO₂ particles. Next, characterization was done to Cu/TiO₂ particles using Field-Emission Scanning Electron Microscope (FESEM) for surface morphology, using Energy-Dispersive X-ray spectroscopy (EDX) for elemental composition, using X-Ray Diffraction (XRD) for phase identification analysis and using Zeta Potential for surface charge.

In second phase, the photocatalytic properties of these particles were determined via photodegradation of RhB. The result was evaluated via UV-Visible Spectrophotometer. The data sampling in this study was based on Taguchi method. The synthesis parameters studied were optimized for the poorest photocatalytic performance using DOE via Taguchi method. The

transmittances of the pure thin silicone film and thin silicone film incorporated with TiO₂ particles as well as Cu/TiO₂ particles after exposure to UV irradiation were evaluated.

1.5 Dissertation Outline

This thesis consists of five chapters. Chapter One discusses the introduction, objectives, research motivation, problem statements and study scopes of the project. Meanwhile, Chapter Two explains the LED, encapsulant embedded in LED, discoloration of LED encapsulant, basics of TiO₂, development of TiO₂ in the LED encapsulant, surface modification of TiO₂ particles and statistical tool used for optimising the synthesis parameters. Experimental details and characterization approaches are explained in Chapter Three. Moreover, Chapter Four focuses on the result analysis and discussion of this project. Lastly, the conclusion of this project and the recommendations of future work are indicated in Chapter Five.

CHAPTER 2

LITERATURE REVIEW

This chapter explains the LED, encapsulant embedded in LED, silicone encapsulant discoloration, surface modification of TiO₂ particles and statistical tool used for optimising the synthesis parameters. Besides, it reviews the basics of TiO₂, which its photocatalysis mechanism being applied in the encapsulation of LED. The factors that influenced the photodegradation process are being discussed. On the other hand, discussion is also done on the reflective properties of encapsulant and TiO₂. Moreover, surface modification in improving photocatalytic activity such as coupling of TiO₂ particles, doping of TiO₂ particles, the addition of metal to TiO₂ and surface sensitization of TiO₂ particles are also reviewed in this chapter.

2.1 LED

LED are one of the most recent developments of lighting, which are mostly used in illumination and display areas due to their compact size, cost effectiveness, ability to conserve energy and environmental friendliness (Fan et al., 2021). As LED were developed, the increment in light levels has reached to the extent that they could be considered for more complex applications. High-power LED is a brand-new generation of solid-state lighting technology which known as the fourth generation of light source and they are reshaping the light industry (Zhou et al., 2022; Delendik et al., 2021). Due to its great preparation efficiency, increased brightness, and increased lighting range, high-power LED have been produced (Zhou et al., 2022). Energy consumption is known to be a crucial issue as it has a major impact on global warming (Yazdan et al., 2020). Improvements in energy efficiency, energy system lifespan, and cost reduction are made possible by rising interest in environmental preservation and energy conservation (Seo & Lee, 2018). According to U.S. Department of Energy projections, advanced lighting systems are expected to

save 6.9 trillion kWh of electricity by 2035 if the aims for efficiency, controls, and connected lighting are achieved. The total cumulative energy savings involving \$710 billion in avoided energy costs and 2.1 billion metric tons of avoided carbon dioxide emissions (*About the Solid-State Lighting Program, 2022*). The size of the worldwide LED lighting market was estimated at USD 50.91 billion in 2020, and it is projected to reach USD 59.26 billion in 2021 and USD 135.58 billion in revenue in 2028. From 2021 to 2028, there should be a 12.5 percent compound annual growth rate (*LED Lighting Market Share & Growth Report, 2021-2028, 2021*). The growing need for energy-efficient lighting solutions, declining LED prices, and escalating infrastructure development projects are likely to be the causes of the rising in the worldwide LED lighting market size (*P&S Intelligence, 2021*).

According to researchers, application efficiency, which can describe the effective conveyance of light from the light source to the lighted task, is said to be the next generation of solid-state lighting energy savings (Pattison et al., 2017). As compared to other available lighting sources, LEDs have the lowest energy consumption per lumen produced (Yazdan et al., 2020). Luminance, which is used to measure the brightness of displays, describes the brightness of light emitted (passing through or reflecting off a surface per unit area at a solid angle). Luminous efficacy (lumens per watt), which is the proportion of luminous flux to input power, indicated the energy efficiency (Sametoglu & Koc, 2021). Luminous efficacy usually decreases with increment in input power. This is probably due to increment in input power resulting the high heat generated from the LED chip and thus high junction temperature is observed. As a result, the luminous decay rate accelerates and caused the shift of wavelength of lighting colour happened rapidly (Sametoglu & Koc, 2021). Aside from luminous efficacy, other key factors that make LEDs a superior power lighting source include colour rendering index, lifespan, and reliability (Yazdan et al., 2018; Yazdan et al., 2020). The Alliance for Solid-State Illumination Systems and Technologies defines LEDs

lifetime based on the amount of time it takes for its light output to degrade by 50% or 70% at ambient temperature, in which, the lifetime is shown by lumen maintenance (Yazdan et al., 2018).

However, actual lifespan and performances of LEDs are much lower than the expected under the constant impacts of electrical, thermal, chemical or mechanical stress (Lin et al., 2021). The failure modes of LEDs can be categorized according to the LED components, as shown in Table 2.1.

Table 2.1: Failure modes of LEDs (Yazdan et al., 2020)

Components of LED	Identified Failure Modes
Bare die	LED catastrophic failure
	Lumen depreciation
LED packaging	Yellowing of packaging materials
	Electrostatic discharge
	Interconnect failure
	Cracks
	Delamination
	Wire bond failure
LED's on substrate	Cracks
	Solder fatigue
	Printed circuit board metallization
	Short due to solder bridging
LED module	Casing cracks
	Optic degradation
	Electrostatic discharge failures
Luminaire	Fractures

	Moisture related failures
	Driver failures
	Deposition of outgassing material on the optics
Lighting system	Software failures
	Electrical compatibility issues
	Installation and commissioning issues

2.1.1 Working Principle of LED

LED is a new kind of solid-state lighting technology which the semiconductor device will emit light upon the electricity flow, following the principle of electroluminescence (Zhou et al., 2022; Dutta Gupta, 2017). As indicated by *Dutta Gupta*, the LED chip is a small semiconductor wafer with a size of approximately 1 mm^2 , which has been incorporated with specific impurities or dopants. Two categories of dopants can be impregnated into the LED chip, for instance, p-type and n-type dopants. The p-type dopant acts as donor acceptor which have a high concentration of holes (h^+), whereas, the n-type dopant acts as e^- donor that have a high concentration of e^- . In general, LED is a p-n junction diode which the p-type and n-type doped semiconductor crystal are fused together to form a heterojunction, where the light emits in the forward biased (Snehasish & Avinash, 2017; Dutta Gupta, 2017).

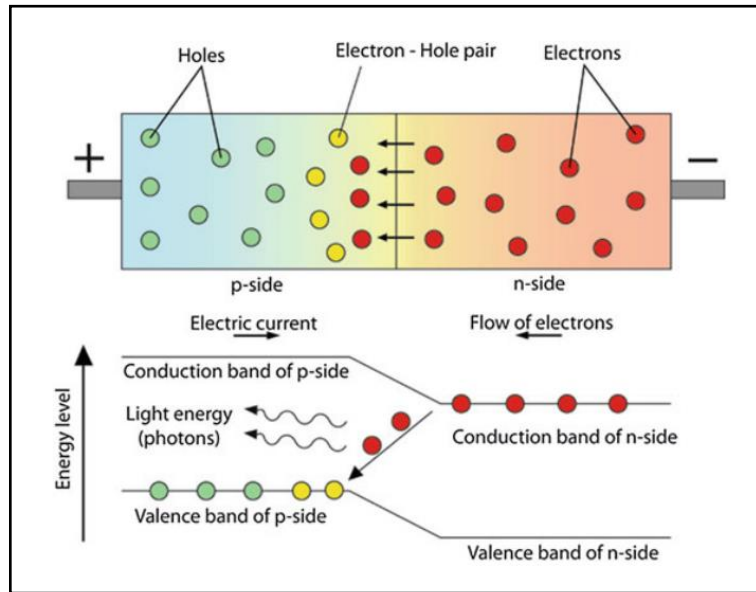


Figure 2.1: Working principle of LED (Snehasish & Avinash, 2017)

The working principle of LED is based on the quantum theory. According to quantum theory, the e^- falls from a higher energy level to a lower energy level will result in emission of photon energy, which correspond to the energy band gap between two energy levels. In a simple way, as shown in Figure 2.1, e^- and h^+ will move across the p-n junction. The e^- will fall into the vacant spaces and eventually combined to form electron-hole pairs to travel from conduction band (CB) to valence band (VB). The flow of charge carriers is known as recombination, where light is generated (Snehasish & Avinash, 2017). The excess energy is released as electromagnetic radiation with a certain wavelength or colour that corresponds to the difference in valence shell energies of the p-type and n-type dopants because the newly acquired orbital energy is lower than the energy possessed by the e^- (Dutta Gupta, 2017).

2.1.2 Encapsulant embedded in LED

An LED package comprises of a LED chip (microelectronic components), an adhesive (die bonding paste), an encapsulant, a fluorescent substance (semiconductor), heat-radiant material (reflector) and interconnects (electric wires), as shown in Figure 2.2 (Masui et al., 2016; Chung et al., 2014). It is important to ensure the microelectronic components are provided with protection

against the aggressive system and environmental stress (Yazdan et al., 2020). The LED encapsulant is a vital element which it is embedded in the LED packaging for two main functions, which are mechanical and environmental protection, and also high light-extraction (Masui et al., 2016). It acts as a protective layer which able to avoid bond wire detachment, external vibrations, chemical pollution and even moisture (Baillot et al., 2015). Selection of encapsulant materials is crucial for the performance of LEDs. The chosen encapsulant material should portrays favourable high temperature stability, high stability towards high photon fluxes that occur within LEDs, high optical transparency, high refractive index, good adhesion, good mechanical properties, chemical stability, and hermeticity (Yazdan et al., 2020; Wang et. al., 2014).

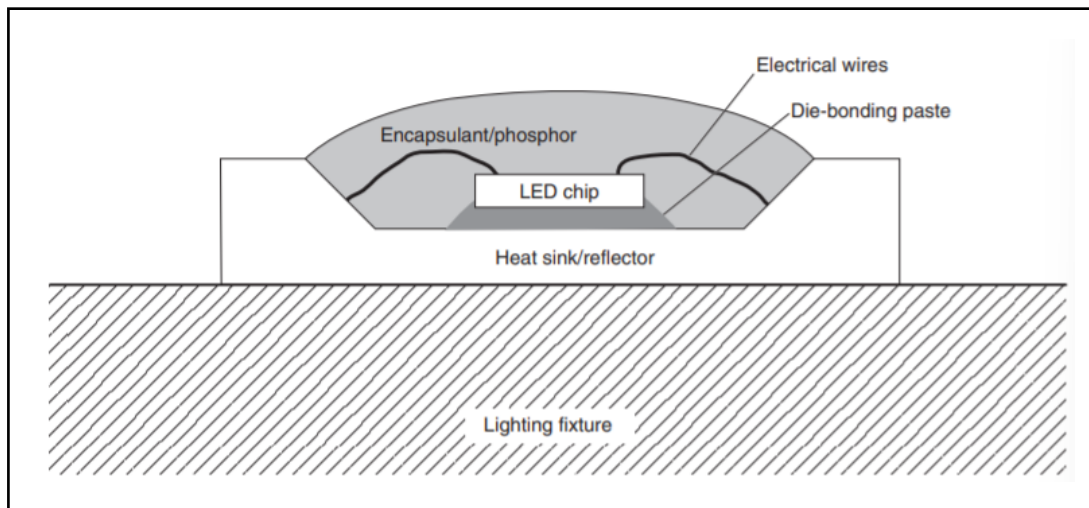


Figure 2.2: Cross-sectional view of high-power white LED (Masui et al., 2016)

Nowadays, various encapsulant materials are being adapted into LED packaging, such as epoxy resin, silicone resin, silica glass, phosphor, ethyl vinyl acetate, polyimides and polymethyl methacrylate, which their excellent transparency, high refractive index, long-term thermostability and aging resistance are essential elements (Lin et al., 2021; Lee, 2000). Among the variety of materials mentioned, epoxy resin and silicone resin are the commonly suggested materials for an LED encapsulant resin, as they have high resistance to yellowing/browning (Chung et al., 2014; Baillot et al., 2015).

Silicone-based polymer is preferably used as an encapsulant material for surface-mount LEDs due to its excellent thermal stability ($> 180\text{ }^{\circ}\text{C}$), good insulation to moisture, high transmittance ($> 95\%$ in the blue range), good homogeneity to minimize scattering and high transparency (Huang et al., 2015; Baillot et al., 2015). Siloxane-based polymers are commonly used as coatings in the optical electronic industry, to be specific, terminated silicone, tri-methyl-silyloxy, poly(dimethyl siloxane) and poly(methyl-phenyl-siloxane) (Baillot et al., 2015; Yazdan et al., 2020). Various ratio of methyl to phenyl units can be made to obtain refractive indices from 1.40 to 1.55. As compared to epoxy-based polymers, silicone-based polymers are more durable against blue and UV rays (Chung et al., 2014). However, challenges remained regarding the wavelength sensitivity in the near UV/blue range and temperature although silicone-based polymers have negligible light loss in the range from 400 nm to 1310 nm (Baillot et al., 2015). Unfortunately, silicone-based polymers have low RI, approximately 1.4 to 1.5 which limits the LEE. To overcome this issue, a reduced index contrast at the semiconductor interface may subsequently increases the internal total reflection angle, thereby improving LEE (Baillot et al., 2015). Besides, the gas barrier properties of silicon based encapsulants are poor, thus degradation of elements or corrosion of electrodes may be produced (Chung et al., 2014).

On the other hand, epoxy-based polymer is also a popular candidate for the encapsulant materials due to its ability to resist moisture, ease of manufacturing and good mechanical stability (Yazdan et al., 2020). However, as one of the encapsulant materials, they are known to have two major short comings. Unlike silicone-based polymers, epoxy-based polymers are prone to photodegradation under UV radiation and high temperatures up to $260\text{ }^{\circ}\text{C}$. Massive chain scission is said to take place, causing the fast discoloration of encapsulant happened, indicating they have poor thermal stability (Ibrahim Khalilullah et al., 2018; Yazdan et al., 2020). Besides, there is also a high possibility for excessive crosslinking to occur that resulting brittleness in the material itself.

Table 2.2 shows the comparison between the properties of silicone resin and epoxy resin. Modifications on encapsulant material is then studied accordingly with the introduction of dopants into silicone.

Table 2.2: Comparison of the properties of silicone resin and epoxy resin

Type of encapsulant		Properties	References
Silicone	Benefits	<ul style="list-style-type: none"> • Excellent thermal stability • High transparency • Excellent oxidative stability • Excellent yellow-resistance • Durable against blue and ultraviolet rays • Lower flammability • High power resistance 	(Huang et al., 2015), (Lin et al., 2021), (Chung et al., 2014), (Beaucarne et al., 2021), (Lin et al., 2018)
	Consequences	<ul style="list-style-type: none"> • Low RI (1.4-1.5) • High gas permeability • Weak adhesion strength • Soft materials • High thermal expansion coefficient (CTE) match to LEDs • High cost • Low volatiles distribution in production area 	(Chung et al., 2014), (Lin et al., 2021), (Lin et al., 2018)
Epoxy	Benefits	<ul style="list-style-type: none"> • Low cost • Robust mechanical property • Strong adhesion strength • Good moisture resistance • Good chemical resistance • Good thermal expansion coefficient (CTE) match to LEDs • Moderate RI (1.5) 	(Lin et al., 2021), (Lin et al., 2018)

		<ul style="list-style-type: none"> • Hard materials 	
	Consequences	<ul style="list-style-type: none"> • Limit thermal stability • Weak photo-resistance 	(Lin et al., 2018)

2.1.3 Yellowing/Browning (Discoloration) of LED Encapsulant

Encapsulants provide protection to LED from physical and environmental attacks, as well as providing the necessary mechanical strength by adhering the individual parts of the module properly to each other. However, conditions such as high radiation doses, large temperature gradients, high seasonal humidity and high ambient temperature might result photodegradation of polymeric materials (Correa-Puerta et al., 2021). Photodegradation as one of the major causes for the LED failures, will lead to reduction in transparency, transmission losses, delamination and discoloration (Yazdan et al., 2020; Correa-Puerta et al., 2021).

The encapsulant photodegradation plays a vital role in determining the lifespan and reliability of the LEDs. It is found to be the dominant cause for lumen degradation of LEDs in conditions of elevated temperature and humidity (Singh & Tan, 2018). Taking silicone as the prominent encapsulant material, the progression of the degradation starts from the hydrolysis of the silicone, then condensation, followed by thermal oxidation and lastly thermal aging (Singh & Tan, 2018). Cai et al. indicates that one of the important degradation mechanisms is the aging of the optical materials. Under typical operating settings, optical and thermal failure mechanisms that had an impact on the molecular structure of the polymer could impair the optical performance of LED (Baillot et al., 2015). In fact, thermal oxidation is the crucial mechanism which leads to the silicone photodegradation. Due to applications of high-power LED, silicone will tend to degrade via chemical degradation upon exposure of elevated temperatures (as high as 135 °C) and at increased levels caused degradation rates to increase further (Yazdan et al., 2020; Singh & Tan, 2018; Appaiah et al., 2015). Silicone will undergo chemical structure change through mechanisms such as chain

scission and oxidation. This phenomenon will lead to the encapsulant materials discoloration, eventually producing an increased absorption of blue light (Yazdan et al., 2020). Moreover, increment in mechanical strength and cracks initiation can be observed under high temperature conditions (Singh & Tan, 2018).

At the same time, silicone photodegradation that caused discolouration of encapsulant depends on the exposure duration and intensity of radiation (Yazdan et al., 2020). The inconsistent degradation of wavelength-dependent transmittance caused the nature of oxidation process encourages the lowering of the blue/yellow light intensity ratio, where the colour shift occurs towards yellow field (Lu et al., 2015). The increase in blue photon absorption can be attributed to the discoloration of LED encapsulant, which results in a change in the blue-emission peak shape and a shift of the emission peak to longer wavelengths. (Davis, 2017). Contradictorily, *Yazdan et al.* reported that temperature has a greater contribution to the discolouration than the short-wavelength radiation. Under the influence of elevated temperature and radiation exposure, photodegradation which leads to discolouration is found to be the dominant cause for the colour shift and lumen depreciation of LEDs (Yazdan et al., 2018; Singh & Tan, 2018). The spectral power distribution and yellowing index of the degraded specimens that using measurement from integrated sphere are always good measures of the discoloration specimens (Yazdan et al., 2018).

2.2 Basics of TiO₂

TiO₂ is a well-known photocatalyst due to its promising properties, involving stability, non-toxicity, biocompatibility, low cost, reusability, eco-friendliness, optical and electrical properties (Nyamukamba et al., 2018; Pawar et al., 2018). A variety of method can be used to synthesize TiO₂, including hydrothermal (Keerthana et al., 2018; Nyamukamba et al., 2018), sol-gel (Behnajady & Eskandarloo, 2015; Nyamukamba et al., 2018), spray pyrolysis (Nyamukamba et al., 2018),

microwave-assisted (Nyamukamba et al., 2018) and plasma enhanced chemical vapour deposition (Borras et al., 2020).

TiO₂ usually exists as an n-type semiconductor due to the occurrence of oxygen vacancies (Pawar et al., 2018). It is a polymorphic material, which has phases of anatase, rutile and brookite (Allen et. al., 2018). The crystal structure of TiO₂ polymorphs can be indicated via different spatial arrangements of TiO₆ octahedra, which Ti⁴⁺ ions are bordered by six O²⁻ ions (Etacheri et al., 2015). Different degrees of distortion is the crucial aspect of the different spatial arrangements of TiO₆. Anatase, rutile and brookite are the common polymorphs of TiO₂, as shown in Figure 2.3. In anatase, there is no edge sharing, yet each octahedron shares four of its corners. It has tetragonal crystal structure, which can be viewed as zigzag chains of the octahedra connected together through corner sharing (Allen et. al., 2018). It is always the first TiO₂ phase to be formed, as its surface energy is low, which will then be transformed to rutile when heated (Hanaor & Sorrell, 2010). Meanwhile, rutile has two opposing edges of an octahedron are shared to form linear chains along the edge direction (Allen et. al., 2018). It has a tetragonal crystal structure and exhibits low total free energy, thus it is unable to transform to other phases. On the other hand, brookite has octahedrons which share both edges and corners, forming an orthorhombic structure (Allen, 2018). It presents in the form of tabular, elongated and striated parallel to their length. It is not commonly found and usually occurs as a by-product.

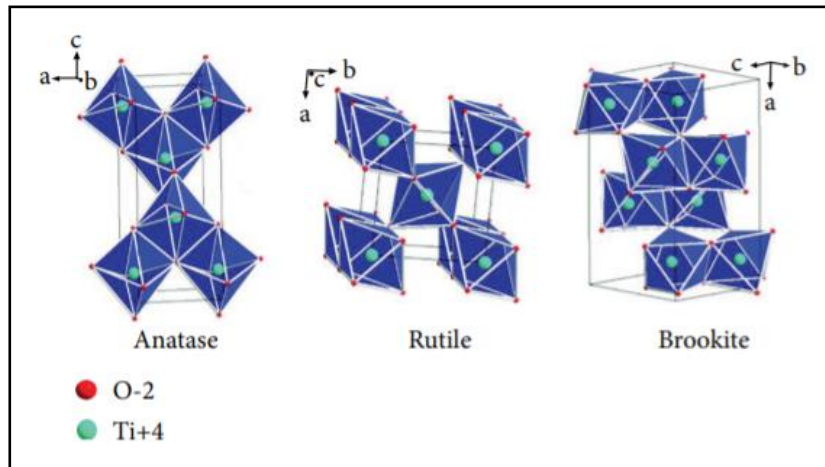


Figure 2.3: Different crystal structure of TiO₂ polymorphs: (a) anatase, (b) rutile, and (c) brookite

(Pawar et al., 2018)

The properties of TiO₂ greatly depends on its polymorphs, as shown in Table 2.3. Rutile is the most thermodynamically stable phase, which is easily obtained through annealing; meanwhile anatase and brookite are metastable, which can be transformed irreversibly and exothermically to rutile at elevated temperatures exceeding 600 °C (Etacheri et al., 2015). Rutile is commonly used as white pigment in paint, whitener in toothpaste and UV absorber in sunscreens; while anatase (in nanocrystalline form) is used as a photocatalyst, a dye-supporting electron-transporting substrate in solar cells and also an active component in self-cleaning cement (Zallen & Moret, 2006). In the photocatalytic aspect, anatase portrays greater performance due to the superior mobility of electron-hole pairs. In contrast, photocatalytic performance of rutile is not promising, while brookite is not systematically investigated (Etacheri et al., 2015).

Table 2.3: Properties of the TiO₂ polymorphs

Properties	Anatase	Rutile	Brookite	References
Band gap energy (eV)	3.2	3.0	3.4	(Pawar et al., 2018), (Umar & Abdul, 2013), (Lance, 2018), (Samat et al., 2017), (Coronado et al., 2013)
Wavelength (nm)	385 - 388	413 - 415	-	(Umar & Abdul, 2013), (Nyamukamba et al., 2018)
Transition	Direct/ Indirect	Direct	Direct/ Indirect	(Zallen & Moret, 2006), (Samat et al., 2017), (Coronado et al., 2013)
RI	2.55	2.73	-	(Kemp & McIntyre, 2001), (Nyamukamba et al., 2018)
Molecular Weight (g/mol)	79.88	79.88	79.88	(Nyamukamba et al., 2018)
Melting Point (°C)	1825	1825	-	(Nyamukamba et al., 2018)
Boiling Point (°C)	2500 - 3000	2500 - 3000	-	(Nyamukamba et al., 2018)
Specific Gravity	3.9	4.0	-	(Nyamukamba et al., 2018)
Light Absorption (nm)	≤ 385 nm	≤ 415 nm	-	(Nyamukamba et al., 2018)
Mohr's Hardness	5.5	6.5 – 7	-	(Nyamukamba et al., 2018)
Dielectric Constant	31	114	-	(Nyamukamba et al., 2018)
Crystal Structure	Tetragonal	Tetragonal	Orthorhombic	(Allen, 2018), (Nyamukamba et al., 2018)
Lattice Constants (Å)	a = b = 3.7845; c = 9.5143	a = b = 4.5936; c = 2.9587	a = 5.4558; b = 9.1819; c = 5.1429	(Pawar et al., 2018), (Etacheri et al., 2015), (Nyamukamba et al., 2018)
Density (g/cm³)	3.79	4.13	3.99	(Nyamukamba et al., 2018), (Pelaez et al., 2012)
Particle Size (nm)	> 35	< 11	11 - 35	(Pawar et al., 2018)

2.3 Performance of TiO₂ Particles as Filler in the LED Encapsulant

LED encapsulant provides physical protection to LEDs and contributes to higher light output due to its reflector shape and special filler addition (Singh & Tan, 2018). Incorporation of inorganic nanoparticles into encapsulant materials as a filler is an effective way to enhance mechanical and physical properties of transparent polymers, such as strength, stiffness, thermal expansion coefficient, thermal conductivity, UV-shielding and UV-resistance (Li et al., 2008).

Li et al. reported that it is acceptable if the optically transparent nanocomposites have the same transparency as the polymer matrix, which indicating the refractive index perfectly matches between the inorganic nanocomposite fillers and the polymer matrix ($n_p = n_m$). Nevertheless, the RI is an intrinsic material property. It is quite hard to maintain the high transmittance of transparent polymer matrices as the refractive index of inorganic nanocomposite fillers is greatly differ from the polymer matrix. The refractive index mismatch between the inorganic nanocomposite fillers and the polymer matrix is a common phenomenon, which would inevitably lead to light scattering happens that subsequently result in opaqueness even if the filler content is low. In order to minimize scattering losses, incorporating fine particles 1-2 orders of magnitude smaller than wavelength of light is preferred. However, particle agglomeration becomes severe with the reduction of particle size, which then deteriorates the particle dispersion in the polymer matrix. The agglomeration persists in the polymer matrix and scatter visible light, resulting turbidity. Anyhow, core-shell structured particles are suggested by assuming that they have one refractive index in the polymer medium. In principle, high transparent polymer nanocomposites are possible to obtain via introduction of core-shell structured particles with the same RI as that of the transparent polymer matrix (Li et al., 2008).

The silicone encapsulation shown in Figure 2.4 (a) employed in the high-power LEDs has limited refractive index, which leads to low LEE of LEDs due to the large RI difference between

silicone encapsulant and LED chips (Wang et al., 2014). Semiconductors such as TiO₂, zinc oxide (ZnO), zinc sulphide (ZnS), tungsten trioxide (WO₃) and cadmium sulphide (CdS) are the common heterogeneous photocatalysts which promotes photocatalytic performance (Sushma & Yadav, 2020). With the elements introduced into the LED encapsulant, the problems previously stated can be solved. TiO₂ is recommended among the photocatalysts due to its low cost, high stability, excellent charge transportation ability and environmental friendliness (Sushma & Yadav, 2020; Qureshi et al., 2020). *Jain and Vaya* reported that high surface-volume ratio of TiO₂ particles offers an increase in light absorption rate, subsequently increasing the surface photo-induced carrier density which leads to higher surface photoactivity and enhanced photocatalytic activity of TiO₂ particles. This is due to a smaller crystallite size of doped TiO₂ nanoparticles induced a larger band gap due to the increment in redox ability. Moreover, the quantum size effect of doped TiO₂ nanoparticles increases its photocatalytic activity. TiO₂ particles should be mesoporous and should exhibit high crystallinity and specific area in order to achieve high photocatalytic degradation efficiency. Vice versa, low photocatalytic degradation may be achieved with core-shell structured TiO₂ particles

As shown in Figure 2.4 (b), modified encapsulant was fabricated by doping elements (TiO₂) into silicone. As reported by *Huang et al.*, the effect of TiO₂ on the durability was investigated by evaluating the long-term stability of the LED module, which is shown in Figure 2.5. With the evaluation controlled at 85°C/85 % relative humidity (RH) and under continuous bias mode, it is found that the durability of the LED modules incorporated with silicone/TiO₂ encapsulant is greater as compared to pure silicone encapsulant. The relative intensities of the emission are retained as high as 96.2 %, which indicates the introduction of TiO₂ into silicone encapsulant brings no harm on the long-term stability of the LED module (Huang et al., 2015). In general, TiO₂ is known to be a promising semiconductor due to its high performance in photocatalytic applications. The white

pigment in TiO₂ is extensively used as absorbing pigment in the photocatalytic activity due to its hydrophobicity (Sushma & Yadav, 2020).

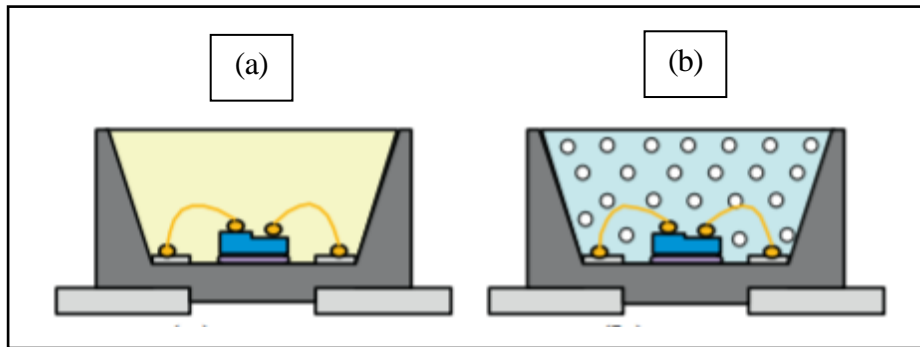


Figure 2.4: LED encapsulant: (a) silicone and (b) TiO₂ doped silicone (Wang et al., 2014)

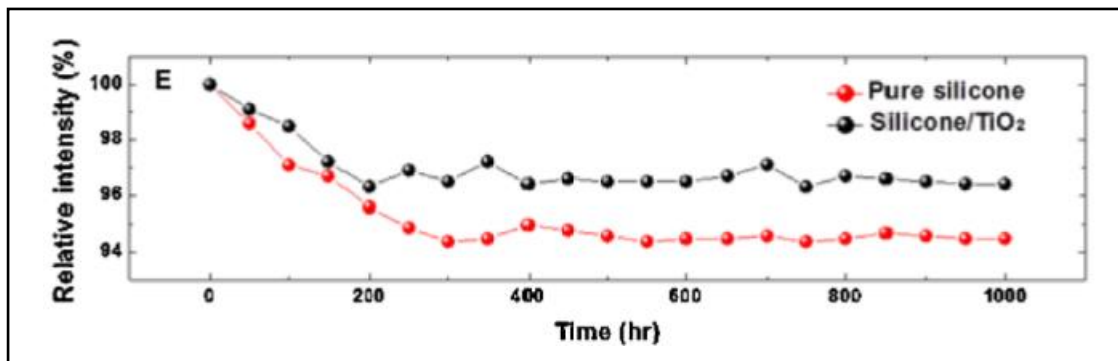
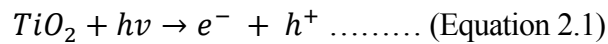


Figure 2.5: Durability test for the LED module with different packages under 85 °C/85 % RH condition (Huang et al., 2015)

2.3.1 Photocatalytic Activity of TiO₂

Electronic structure of a semiconductor plays an important role in photocatalysis, which refers to the acceleration of the chemical reaction via the aid of photocatalysts. The energy difference between CB and VB, or so-called band gap, is crucial to determine the feasibility of the redox reaction to occur. TiO₂ with a band gap of 3.0 eV to 3.4 eV (different phase of TiO₂ portrays different band gap, may refer Table 2.2), is a common semiconductor that is selected as photocatalysts. However, electronic structure of TiO₂ has a wide band gap, which consists of unoccupied CB and occupied VB (Etacheri et al., 2015). This indicates high energy of photons with short wavelength (such as UV light or blue light, where wavelength < 388 nm) is required to favour the redox reaction.

In fact, photocatalytic performance of TiO₂ is manipulated by the photogeneration of charge carriers correlated to the band gap. In heterogeneous photocatalysis, UV light is absorbed on to the surface of the TiO₂, where redox reaction takes place. As shown in Figure 2.6, an e⁻ is excited from VB towards CB upon sufficient photon energy initiated by UV light absorption. In response, electron-hole pairs are produced due to the formation of h⁺ in the VB and e⁻ in CB, as shown in following Equation 2.1:



The e⁻ in the CB and the resultant h⁺ in the VB are good reducing agents and strong oxidizing agents respectively (Haider et al., 2017; Moma & Baloyi, 2019). Both e⁻ and h⁺ are then migrated to the surface of TiO₂ and participate in redox reactions with their strong redox ability (Zhang *et al.*, 2017). In fact, redox reactions are not necessary happen on the surface of the TiO₂, but also at the bulk of TiO₂, as shown in Figure 2.7. Figure 2.6 shows the different pathways for the separation of e⁻ and h⁺, where h⁺ can oxidize the donor species (pathway a) while e⁻ can reduce the donor species (pathway b). However, charge carriers are not necessarily undergo charge transfer to adsorb species, possibly recombination process instead. The separated e⁻ and h⁺ are recombined (pathway c or d), resulting the photon energy is converted into heat and released (Linden & Mohseni, 2014). This eventually reduced the photocatalysis efficiency of TiO₂. TiO₂ is employed in a wide range of applications including photocatalysis, pigments, dye sensitized solar cells, air/water sanitization, optoelectronics, cancer therapy, cathodic protection of metals from corrosion and light-activated antibacterial surfaces (Etacheri et al., 2015).

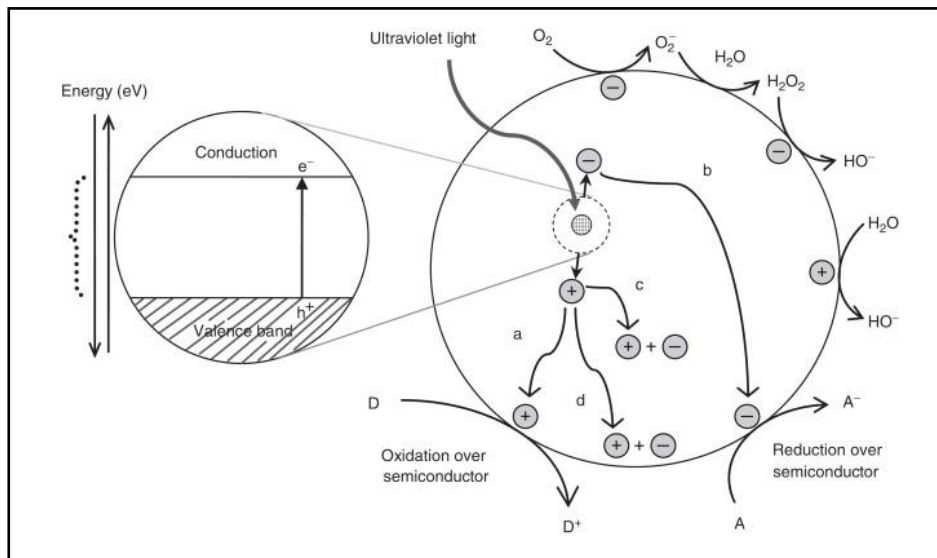


Figure 2.6: Schematic diagram of photocatalysis (Linden & Mohseni, 2014)

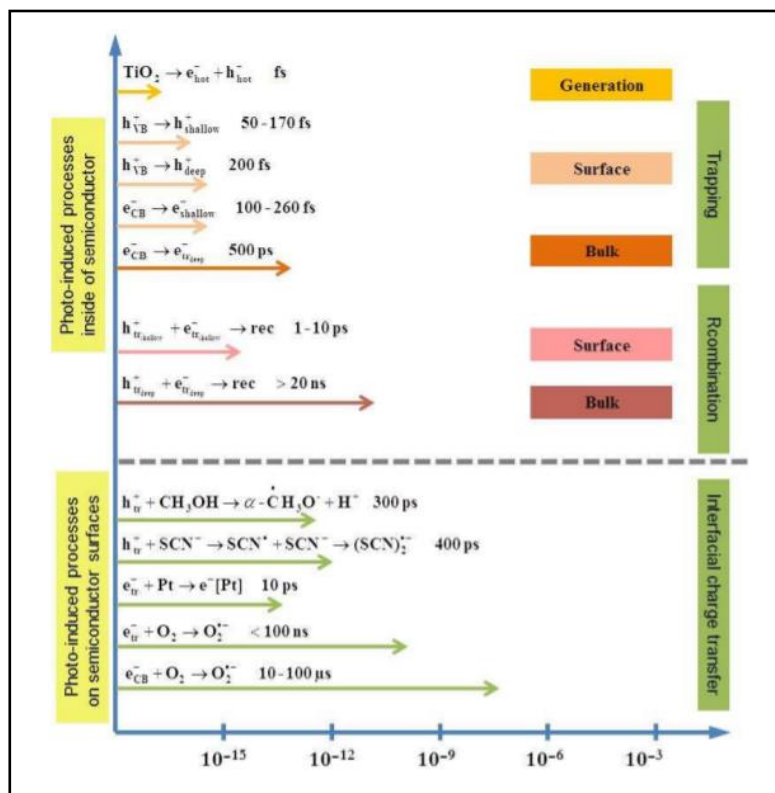


Figure 2.7: Various reactions involved in TiO_2 photocatalysis (Etacheri et al., 2015)

There are a number of factors influencing the photocatalytic efficiency of TiO_2 , such as surface area, particle size, ratio of polymorphs, type of dopants, synthesis method, phase purity, intensity of light source, photocatalyst polymorph, temperature and photocatalyst concentration, as shown in Table 2.4.

Table 2.4: Factors influencing the photocatalytic efficiency (Pawar et al., 2018)

Factors	Description
Intensity of light source	Increment in intensity of light improves charge separation, thus increases the photocatalytic efficiency
Photocatalyst polymorph	Different polymorph has different band gap, thus different photocatalytic efficiency can be observed.
Temperature	Increment in temperature reduces the photocatalytic efficiency due to the enhanced electron-hole recombination pairs and enhanced desorption of adsorbed species from the exterior of the photocatalyst.
Photocatalyst concentration	Increment in concentration of the catalyst improves the photocatalytic efficiency. However, specific catalyst concentration has to be determined because the excess catalyst prevents the diffusion of the light into the solution which might result in unfavourable light scattering.
pH of the solution	pH of solution and size of aggregates alter the surface charge properties due to the different charge of the semiconductor surface.

TiO₂ has its limitation as a photocatalyst as it has a wide band gap which inhibited the usage of visible light. Its photocatalytic properties can only be activated when it is exposed to UV light (wavelength ≤ 390 nm). However, its performance is restricted although the absorption onset of rutile ($E = 3.0$ eV) occurs around 413 nm. It subsequently deteriorates the photocatalytic activity due to mediocre redox potential and faster photogenerated recombination of electron-hole pairs (Etacheri et al., 2015; Pawar et al., 2018). Consequently, low quantum yield rate and a limited photooxidation rate can be observed (Huang et al., 2016). Besides, solar light comprises of 5% UV light (300–400 nm), 43% visible light (400–700 nm), and 52% infrared light (700–2500 nm) (Etacheri et al., 2015;